Critical Behavior in Double-Exchange Ferromagnets of $Pr_{0.6}Sr_{0.4}MnO_3$ Nanoparticles

Tran Dang Thanh[1,2], Yu YiKyung[3], T. A. Ho[1], T. V. Manh[1], The Long Phan[4], Daniel M. Tartakovsky[3], and Seong Cho Yu[1]

[1]Department of Physics, Chungbuk National University, Cheongju 361-763, Korea
[2]Institute of Materials Science, Vietnam Academy of Science and Technology, 18-Hoang Quoc Viet, Hanoi, Vietnam
[3]Department of Mechanical and Aerospace Engineering, University of California at San Diego, La Jolla, CA 92093 USA
[4]Department of Physics, Hankuk University of Foreign Studies, Yongin 449-791, Korea

In this paper, we present a detailed study on the critical property around the ferromagnetic (FM)–paramagnetic phase transition of $Pr_{0.6}Sr_{0.4}MnO_3$ nanoparticles (NPs) with different crystallite sizes (d = 39–88 nm), which were synthesized by the combination of the solid-state reaction and mechanical milling methods. The magnetic results show that the samples undergo the second-order phase transition. The values of the Curie temperature (T_C) slightly decrease from 291 to 286 K while the saturation magnetization (M_S) decreases from 89.7 to 76.3 emu/g and the coercivity (H_C) increases from 322 to 585 Oe with decreasing d from 88 to 39 nm, respectively. Based on the modified Arrott plot method and the isothermal magnetization data around T_C, we have determined the values of critical exponents (β, γ, and δ) and T_C for the samples. The critical exponents $\beta = 0.486 - 0.495$, $\gamma = 1.009 - 1.042$, and $\delta = 3.038 - 3.118$ obtained are close to those expected for the mean field theory ($\beta = 0.5$, $\gamma = 1$, and $\delta = 3$). This proves that long-range FM interactions are present in the NPs. Furthermore, β values are smaller than 0.5, indicating the existence of magnetic inhomogeneity in the NPs. Besides the investigation into the critical behavior, the magnetocaloric effect of the NPs is also investigated.

Index Terms— **Critical behavior, ferromagnetic (FM) interactions, manganite nanoparticles (NPs).**

I. Introduction

IN RECENT years, perovskite-type manganites ($REMnO_3$ with RE = rare-earth elements) have attracted considerable interest due to their complex magnetic and transport properties. Though $REMnO_3$ is an antiferromagnetic (AFM) insulator, substituting the RE site by a divalent alkali earth element (A) in order to form $RE_{1-x}A_xMnO_3$ compounds usually exhibits unusual magnetoelectro effects, such as colossal magnetoresistance [1] and magnetocaloric (MC) effects [2]. Basically, a close interplay between the magnetic and transport properties in $RE_{1-x}A_xMnO_3$ materials is ascribed to the competition between Mn^{3+} and Mn^{4+} FM double-exchange (DE) interactions and AFM superexchange interactions of Mn^{3+}–Mn^{3+} and Mn^{4+}–Mn^{4+} pairs. The magnetic property of $RE_{1-x}A_xMnO_3$ compounds strongly depends on the strength of DE interaction. The doping at the RE/A and/or Mn site is of great importance in modifying the DE strength [1], [3]. In addition, when the particle size of the manganites is reduced to the nanometer scale, a number of outstanding physical properties (such as surface spin-glass behavior, exchange bias effect, superparamagnetism, low saturation magnetization, and large coercivities) will appear [4].

Previous reports have shown some materials exhibiting the giant MC effects with the large magnetic entropy changes (ΔS_m), which are related to structure changes. This phenomenon is known as a first-order phase transition (FOPT) [5]. Nevertheless, the FOPT materials have two important drawbacks, namely, the narrowness of the phase transition region and the presence of the thermal and magnetic hysteresis, which limit their applicability [6]. Some magnetic materials with a second-order phase transition (SOPT) do not exhibit such large ΔS_m values, but their refrigerant capacity (RC) values can be larger than those for FOPT materials due to a wide phase transition. In addition, the hysteresis in the SOPT materials is very small or negligible.

To further understand the magnetic properties in manganite nanoparticles (NPs), it is necessary to consider the influence of the crystallite size (d) on the FM order and the correlation between the MC effect and the critical behavior near the SOPT. In this report, we present a detailed study on the critical properties around FM–paramagnetic (PM) phase transition of $Pr_{0.6}Sr_{0.4}MnO_3$ (PSMO) NPs with different crystallite sizes. We point out the existence of a long-range FM order in PSMO NPs, and their $\Delta S_m(T, H)$ data follow a master curve behavior.

II. Experimental Details

To prepare the PSMO NPs, first, a polycrystalline PSMO bulk was prepared by the solid-state reaction method. High-purity powders (3N) Pr_2O_3, $SrCO_3$, and Mn combined in stoichiometrical quantities were ground and mixed, and then calcinated at 1200 °C for 24 h in air. The obtained mixtures were reground and pressed into pellets and sintered at 1300 °C for 48 h in air. The obtained product was ground in powder, and then used for the mechanical ball milling (used the zirconia-grinding medium of balls and a vial supplied by SPEX-SamplePrep). The milling time (t_m) was chosen to be 10, 20, and 30 min to achieve three samples of PSMO NPs with different crystallite sizes. The ball-to-powder mass ratio was maintained at 4.1. Before milling, the coating was carried out to minimize the unexpected impurities generated from the vial and the balls. The crystal structure of all PSMO samples were checked by an X-ray diffractometer (Bruker

Manuscript received March 19, 2015; accepted April 15, 2015. Date of publication April 21, 2015; date of current version October 22, 2015. Corresponding author: S. C. Yu (e-mail: scyu@chungbuk.ac.kr)

Color versions of one or more of the figures in this paper are available online at http://ieeexplore.ieee.org.

Digital Object Identifier 10.1109/TMAG.2015.2424978

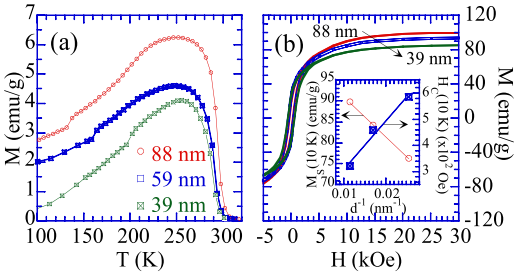

Fig. 1. (a) $M(T)$ curves at $H = 100$ Oe. (b) $M(H)$ curves at 10 K for PSMO NPs. Inset: M_S and H_C at 10 K versus d^{-1}.

AXS, D8 Discover) using a Cu-K_α radiation source ($\lambda = 1.5406$Å). Magnetization versus temperature and magnetic-field measurements were performed on a superconducting quantum interference device magnetometer.

III. Results and Discussion

The room temperature X-ray diffraction (XRD) patterns (not shown) indicated that all the samples are single phase with orthorhombic structure, belonging to the space group, *Pbnm*, without any trace of secondary phases. Based on the XRD data, the lattice parameters calculated ($a \approx 5.48$Å, $b \approx 5.47$Å, $c \approx 7.75$Å, $c/a \approx 1.41$) are almost unchanged with increasing t_m from 10 to 30 min. However, with increasing t_m, the diffraction intensity gradually reduces while the linewidth of the diffraction peaks enhances remarkably. This is due to the reduction of the crystallite size and to the increase of lattice strain (ε) and surface defect density. According to the Williamson–Hall method [7], the average values of the d and ε can be obtained from the intercept and the slope of the following relation $\beta_S \cos\theta = (K\lambda/d) + 2\varepsilon \sin\theta$, respectively, where β_S is the full-width at half-maximum (FWHM) of an XRD peak, θ is the Bragg angle, and $K = 0.9$ is the shape factor. The average values of d and ε are found to be $d = 88$, 59, and 39 nm and $\varepsilon = 0.017$, 0.029, and 0.037 for $t_m = 10$, 20, and 30 min, respectively. Following the contents, we shall only use the parameter d instead of using the milling time t_m.

Fig. 1(a) shows the temperature dependence of the magnetization, $M(T)$, under an applied magnetic field $H = 100$ Oe. All these data were recorded during the warming after zero-field-cooling down to the lowest temperature. One can see that all the samples undergo a FM–PM transition when the temperature increases. The Curie temperature (T_C) was determined from the minimum of the dM/dT versus T curve. T_C slightly decreases from 291 K for $d = 88$ nm to 286 K for $d = 39$ nm.

To get more information related to the magnetic properties of PSMO NPs, we have recorded their magnetic hysteresis loops at 10 K [Fig. 1(b)] and isothermal magnetization $M(H)$ curves at temperatures around the FM–PM phase transition T_C [Fig. 2(a)–(c)] in magnetic fields up to 30 kOe. One can see that the hysteresis loops for PSMO NPs exhibit their soft magnetic behavior with the coercivity (H_C) ~322–585 Oe. While the H_C value increases, the magnetization (M) decreases gradually with decreasing d. It is well-known that the magnetization reduction in the smaller particles is ascribed to the nonmagnetic layer or spin disorder on the particle surface, which lead to the weakening of the Mn^{3+}–Mn^{4+} DE interaction strength [8]. In our case, the value of saturation

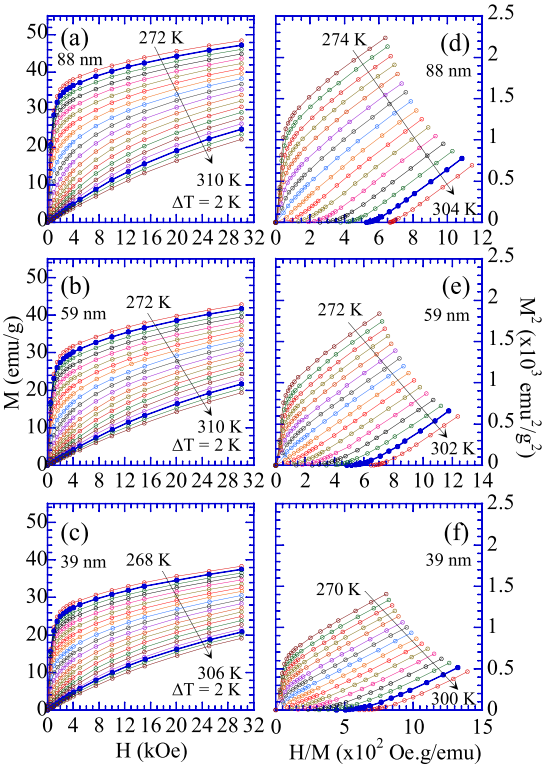

Fig. 2. (a)–(c) $M(H)$ and (d)–(f) M^2 versus H/M curves for PSMO NPs. (a) and (d) $d = 88$ nm. (b) and (e) $d = 59$ nm. (c) and (f) $d = 39$ nm.

magnetization (M_S) obtained at 10 K is reduced linearly with d^{-1} [see the inset in Fig. 1(b)], which confirms that the magnetization is actually influenced by the particle surface.

The $M(H)$ curves around FM–PM phase transition for PSMO NPs [Fig. 2(a)–(c)] show that the magnetization increases most abruptly in weak applied field ($H < 4$ kOe) and then approaches to saturation for above 5 kOe. The saturated magnetization decreases with increasing temperature and proves the purely FM behavior of the samples at $T < T_C$. The nonlinear $M(H)$ curves in the FM state ($T < T_C$) become linear when the material is in the PM state ($T > T_C$) due to the FM–PM transformation. This FM–PM phase transition would be clearer if performing Arrott plots of M^2 versus H/M [9], see Fig. 2(d)–(f). Clearly, the nonlinear parts in the low-field region at the temperature below and above T_C are driven toward two opposite directions, revealing the FM–PM phase separation. The positive slope of the H/M versus M^2 curves (not shown, coordinate axes are the inverse of Arrott plots) reflects all samples undergoing the SOPT, according to Banerjee's criteria [10].

To further understand the nature of FM interactions in PSMO NPs, we have investigated their critical behavior using the modified Arrott plots (MAPs) method [11]. According to the scaling hypothesis, the critical behavior of a continuous phase transition at near the critical temperature T_C can be characterized by set of critical exponents β, γ, and δ, corresponding to the spontaneous magnetization, $M_S(T)$, the inverse initial susceptibility, $\chi_0^{-1}(T)$, and the critical isotherm, respectively, obeying the relations [12]

$$M_S(T) = M_0(-t)^\beta \quad \text{for } t < 0 \tag{1}$$

$$\chi_0^{-1}(T) = (h_0/M_0)t^\gamma \quad \text{for } t > 0 \tag{2}$$

$$M = DH^{1/\delta} \quad \text{for } t = 0 \tag{3}$$

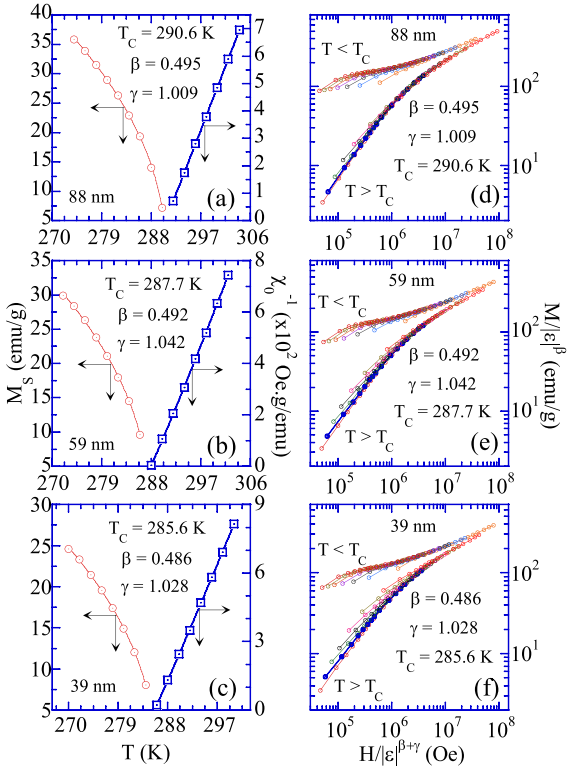

Fig. 3. (a)–(c) $M_S(T)$ and $\chi_0^{-1}(T)$ data (symbols) fitted to (1) and (2) (solid lines), respectively. (d)–(f) $M/|t|^{\beta}$ versus $H/|t|^{\beta+\gamma}$ plots in the log–log scale for PSMO NPs. (a) and (d) $d = 88$ nm. (b) and (e) $d = 59$ nm. (c) and (f) $d = 39$ nm.

where $t = (T - T_C)/T_C$ is the reduced temperature, and M_0, h_0, and D are critical amplitudes. Physically, β describes how the ordered moment grows below T_C, with smaller values indicating faster growth; γ describes the divergence of the magnetic susceptibility above T_C, with smaller values yielding sharper divergence; and δ describes the curvature of $M(H)$ at T_C, with smaller values reflecting less curvature and slower saturation. According to the MAP method [11], with the correct values of β and γ, the performance of $M^{1/\beta}$ versus $(H/M)^{1/\gamma}$ curves is a set of parallel straight lines, and the straight line passes through the origin at the critical point T_C.

The values of $M_S(T)$ and $\chi_0^{-1}(T) = (H/M)(T)$ are determined from the intersections of the linear extrapolation line (for high-magnetic field parts) with the $M^{1/\beta}$ and the $(H/M)^{1/\gamma}$ axes, and are then fitted to (1) and (2), respectively, to achieve new β, γ, and T_C values. These newly found values of β, γ, and T_C are continuously used for the next MAP until getting the stable values of β, γ, and T_C. The $M_S(T)$ and $\chi_0^{-1}(T)$ data fitted to (1) and (2), respectively, with the optimal values of the critical parameters obtained at final step are shown in Fig. 3(a)–(c), with $\beta = 0.486$–0.495, $\gamma = 1.009$–1.042, and $T_C = 285.6$–290.6. Clearly, the value of T_C obtained from the MAP method agrees well with that obtained from the $M(T)$ curve.

For the value of δ, it can be determined directly from the critical isotherm $M(H, T_C)$ following (3). In our case, the value of δ have been determined by fitting the $M(H, T \approx T_C)$ data to (3). The δ values are, thus, found to be 2.934, 2.952, and 3.095 at $T = 290$, 288, and 286 K for PSMO NPs with $d = 88$, 59, and 39 nm, respectively. However, critical exponents (β, γ, and δ) derived from static scaling analysis are related by Widom scaling relation $\delta = 1 + \gamma/\beta$ [12]. Using this relation and the obtained values of β and γ from MAP above, we have calculated $\delta = 3.038$, 3.118, and 3.098 for PSMO NPs with $d = 88$, 59, and 39 nm, respectively. These results are very close to those estimated by critical isotherm $M(H, T \approx T_C)$ analysis.

The reliability of the obtained critical exponents and T_C values can be checked by the scaling hypothesis. According to the prediction of the scaling equation, in the asymptotic critical region, the magnetic equation can be written as [12]

$$M(H, t) = t^{\beta} f_{\pm}(H/t^{\beta+\gamma}) \tag{4}$$

where f_+ for $T > T_C$ and f_- for $T < T_C$ are regular analytic functions. Equation (4) implies that $M/|t|^{\beta}$ as a function of $H/|t|^{\beta+\gamma}$ falls into two universal curves, one for $T > T_C$ and the other for $T < T_C$. For our case, the $M/|t|^{\beta}$ versus $H/|t|^{\beta+\gamma}$ curves in the log–log scale are plotted in Fig. 3(d)–(f) using the critical exponents and T_C values obtained from MAP above. It can be clearly seen that all the $M(H, T)$ data points fall on two universal branches for above and below T_C. This result confirms the values of the critical parameter β, γ, and T_C obtained as described above are believable. However, there is a small deviation of the $M(H, T)$ data from the universal curves at the fields below 3 kOe. This result is related to the rearrangement of magnetic domains, where magnetic moments are not completely aligned to the field.

As mentioned above, the critical exponents for PSMO NPs with $d = 88$, 59, and 39 nm found are $\beta = 0.495$, 0.492, and 0.486; $\gamma = 1.009$, 1.042, and 1.028; and $\delta = 3.038$, 3.118, and 3.098, respectively. It can be clearly seen that these exponents are quite close to those expected for the mean field theory ($\beta = 0.5, \gamma = 1$, and $\delta = 3$) [12]. This means that there exists long-range FM order in the PSMO NPs. However, all the β values obtained are smaller than 0.5, indicating the existence of magnetic inhomogeneities and/or AFM phase on the surface layers of PSMO NPs. Furthermore, the value of β slightly decreases with decreasing d. It reflects that PSMO NPs become more magnetically inhomogeneous when the crystallite size is decreased. This result is ascribed to the increase of surface/volume ratio with decreasing d.

Based on the $M(H)$ data shown in Fig. 2(a)–(c), the MC effect of PSMO NPs can be also assessed via the ΔS_m and RC, which are shown in Fig. 4(a)–(c) and Fig. 4(d), respectively, where ΔS_m is calculated using the Maxwell relation

$$\Delta S_m(T, H) = \int_0^H \left(\frac{\partial M}{\partial T}\right)_H dH \tag{5}$$

and RC $= |\Delta S_{\max}| \cdot \delta T_{\mathrm{FWHM}}$, where $|\Delta S_{\max}|$ and δT_{FWHM} are the maxima value and the FWHM of the $-\Delta S_m(T)$ curves, respectively. One can see that, $-\Delta S_m$ reaches the maxima around T_C, and an H increase enhances $-\Delta S_m$. The variation of the $|\Delta S_{\max}|$ versus H is also plotted in the inset of Fig. 4(d). For each H value, the value of $|\Delta S_{\max}|$ decreases while δT_{FWHM} increases remarkably with decreasing d. Therefore, RC reaches the maximum values on the sample with $d = 59$ nm [Fig. 4(d)]. Namely, under $H = 30$ kOe, the values of $|\Delta S_{\max}|$ are found to be 3, 2.6, and 2.1 $\mathrm{J \cdot kg^{-1} \cdot K^{-1}}$, corresponding to RC = 93, 124, and 103 $\mathrm{J \cdot kg^{-1}}$ for $d = 88$, 59, and 39 nm. These values are comparable with those of some maganites [2], [13], [14] in the same magnetic field change, suggesting that the PSMO NPs can be used for room temperature magnetic refrigeration.

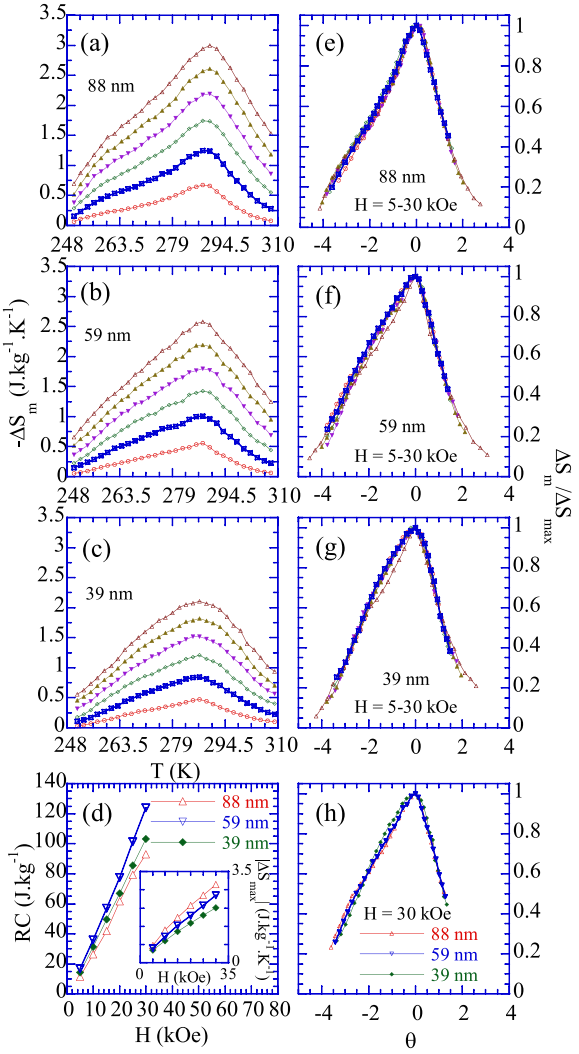

Fig. 4. (a)–(c) $-\Delta S_m(T)$ curves. (d) Variation of the RC versus H. Inset: variation of the $|\Delta S_{\max}|$. (e)–(h) Universal master curves, $\Delta S_m/\Delta S_{\max}$ versus θ for PSMO NPs. (a) and (e) $d = 88$ nm. (b) and (f) $d = 59$ nm. (c) and (g) $d = 39$ nm.

Fig. 4(e)–(h) shows the normalized entropy change for PSMO NPs measured at different temperatures and field changes as a function of the rescaled temperature $\theta = (T - T_C)/(T_r - T_C)$, where T_r is the reference temperature corresponding to a certain fraction k that fulfills $\Delta S_m(T_r)/\Delta S_{\max} = k$. The choice of k does not affect the actual construction of the universal curve, as it implies only proportionality constant [15]. In this paper, T_r values have been selected as $k = 0.6$. Clearly, all the $\Delta S_m(T)$ data points are collapsed onto a single master curve, revealing universal behavior in PSMO NPs. The existence of the universal curve of $\Delta S_m(T)$ under different applied magnetic field changes is an additional confirmation of the general validity of the treatment in SOPT materials. Furthermore, this result also implies that our samples have the same nature of phase transition and follow the same universality class (namely, the β, γ, and δ values are very close to those expected for the mean field theory [12]), as described above [15], [16].

IV. Conclusion

We have studied carefully the critical behavior and MC effect of PSMO NPs with $d = 88$–39 nm. The experimental results indicated that the samples are soft FM materials and belong to the SOPT type. Using the MAP method, the critical exponents of samples were obtained. This suggests the existence of the long-range FM order in the NPs. However, the existence of magnetic inhomogeneity in NPs is also observed. The existence of magnetic inhomogeneity together with the decrease of M_S value in NPs are thought to surface-related effects and distortions, which lead to the weakening of the Mn^{3+}–Mn^{4+} DE interaction strength. Though the M_S and $|\Delta S_m|$ values decrease with reducing d, the phase-transition region and δT_{FWHM} enhance remarkably and, thus, widen the working range of PSMO NPs. In addition, a universal master curve for $\Delta S_m(T)$ data measured at different H have been constructed in the whole temperature range. It would provide important information to understand how their MC effect evolves in desired temperature and magnetic-field ranges.

Acknowledgment

This work was supported by the Converging Research Center Program through the Ministry of Science, ICT and Future Planning, Korea, under Grant 2014048835. Some experiments were performed at facilities of the State Key Laboratory at the Institute of Materials Science, Vietnam Academy of Science and Technology.

References

[1] A. P. Ramirez, "Colossal magnetoresistance," *J. Phys., Condens. Matter*, vol. 9, no. 39, p. 8171, 1997.

[2] M.-H. Phan and S.-C. Yu, "Review of the magnetocaloric effect in manganite materials," *J. Magn. Magn. Mater.*, vol. 308, no. 2, pp. 325–340, Jan. 2007.

[3] J. B. Goodenough, "Electronic structure of CMR manganites (invited)," *J. Appl. Phys.*, vol. 81, no. 8, pp. 5330–5335, 1997.

[4] J. F. Ding *et al.*, "Interfacial spin glass state and exchange bias in manganite bilayers with competing magnetic orders," *Phys. Rev. B*, vol. 87, no. 5, p. 054428, Feb. 2013.

[5] D. Kim, B. Revaz, B. L. Zink, F. Hellman, J. J. Rhyne, and J. F. Mitchell, "Tricritical point and the doping dependence of the order of the ferromagnetic phase transition of $La_{1-x}Ca_xMnO_3$," *Phys. Rev. Lett.*, vol. 89, no. 22, p. 227202, Nov. 2002.

[6] M. D. Kuz'min, "Factors limiting the operation frequency of magnetic refrigerators," *Appl. Phys. Lett.*, vol. 90, no. 25, p. 251916, 2007.

[7] G. K. Williamson and W. H. Hall, "X-ray line broadening from filed aluminium and wolfram," *Acta Metall.*, vol. 1, no. 1, pp. 22–31, Jan. 1953.

[8] M. A. López-Quintela, L. E. Hueso, J. Rivas, and F. Rivadulla, "Intergranular magnetoresistance in nanomanganites," *Nanotechnology*, vol. 14, no. 2, p. 212, 2003.

[9] A. Arrott, "Criterion for ferromagnetism from observations of magnetic isotherms," *Phys. Rev.*, vol. 108, no. 6, pp. 1394–1396, Dec. 1957.

[10] S. K. Banerjee, "On a generalised approach to first and second order magnetic transitions," *Phys. Lett.*, vol. 12, no. 1, pp. 16–17, 1964.

[11] A. Arrott and J. E. Noakes, "Approximate equation of state for nickel near its critical temperature," *Phys. Rev. Lett.*, vol. 19, no. 14, pp. 786–789, Oct. 1967.

[12] H. E. Stanley, *Introduction to Phase Transitions and Critical Phenomena*. London, U.K.: Oxford Univ. Press, 1971.

[13] R. M'nassri, N. C. Boudjada, and A. Cheikhrouhou, "Impact of sintering temperature on the magnetic and magnetocaloric properties in $Pr_{0.5}Eu_{0.1}Sr_{0.4}MnO_3$ manganites," *J. Alloys Comp.*, vol. 626, pp. 20–28, Mar. 2015.

[14] R. Thaljaoui *et al.*, "Magnetocaloric effect of monovalent K doped manganites $Pr_{0.6}Sr_{0.4-x}K_xMnO_3$ ($x = 0$ to 0.2)," *J. Magn. Magn. Mater.*, vol. 352, pp. 6–12, Feb. 2014.

[15] V. Franco and A. Conde, "Scaling laws for the magnetocaloric effect in second order phase transitions: From physics to applications for the characterization of materials," *Int. J. Refrig.*, vol. 33, no. 3, pp. 465–473, May 2010.

[16] C. M. Bonilla, J. Herrero-Albillos, F. Bartolomé, L. M. García, M. Parra-Borderías, and V. Franco, "Universal behavior for magnetic entropy change in magnetocaloric materials: An analysis on the nature of phase transitions," *Phys. Rev. B*, vol. 81, no. 22, p. 224424, Jun. 2010.